HARVARD
John A. Paulson
School of Engineering
and Applied Sciences

Comparison of the Ross procedure and an artificial mechanical valve for aortic valve replacement using fluid-structure interaction modeling

George Nageeb[a] and Oskar Nilsson[b]
[a]SEAS department of Bioengineering, Harvard College, Cambridge, Massachusetts
[b]SEAS department of Mechanical Engineering, Harvard College, Cambridge, Massachusetts

Abstract:

Cardiovascular disease is the number one cause of death worldwide and aortic valve defects are among the most common cardiovascular conditions. Aortic stenosis can lead to fatal complications and often requires corrective surgery for valve replacement. Presently, there are two clinical treatment options commonly used by cardiac surgeons: replacement with an artificial mechanical valve and the Ross procedure (replacing the aortic valve with the pulmonary valve). Given the geometric and material differences between the two we can expect different hemodynamic performances, and additional knowledge about the interactions between blood flow and both valve treatment options is necessary. Computational fluid dynamics (CFD) modeling has emerged as a promising approach in evaluating valve hemodynamics although it is not yet largely applied in the clinical realm. In this paper, we use a Fluid Structure Interaction (FSI) technique with a fully-coupled algorithm and arbitrary Lagrangian-Eulerian formulation (ALE) to investigate both artificial and pulmonary valve performance under aortic physiological conditions. Geometries were constructed in COMSOL using realistic aortic root and valve dimensions with realistic material properties derived from previously published literature. FSI modeling and post-processing was also conducted in COMSOL to assess the performance of each valve. Post-processed data included measurement of maximum jet velocity, transvalvular pressure gradient, wall shear stress on leaflets and aortic wall, von mises stress on both sides of the leaflets, and vorticity magnitude. Results were also validated against published valve data. We found that while the pulmonary valve had slightly lower than expected maximum jet velocity and wall shear stress, ultimately its performance more closely mimicked that of a healthy aortic valve. The Mechanical valve, on the other hand, exhibited lower flow and higher transvalvular pressure gradient then expected, mimicking elements of aortic stenosis. It did, however, experience less shear stress on the leaflets suggesting longer durability. Due to the better hemodynamic performance of the pulmonary valve and the danger of blood clotting with the mechanical valve material, we recommend the Ross procedure as the preferential treatment option for valve replacement in most cases.

I. Introduction

Cardiovascular disease (CVD) is the number one cause of death worldwide and accounts for one of every four deaths in the United States [1]. Aortic valve diseases are among the most common cardiovascular defects. The aortic valve separates the left ventricle from the aorta with three semilunar leaflets, and a healthy valve fully opens during ventricular systole and fully closes during ventricular diastole to ensure unidirectional blood flow [2]. Normally, valve leaflets are exposed to complex hemodynamics during the cardiac cycle. The ventricularis side of each leaflet is exposed to unidirectional jet flow at peak systole, while the opposite fibrosa surfaces are exposed to circulatory flow causing the valve to close [3]. Common defects in the aortic valve include congenital bicuspid valve and valve calcification which result in disturbed

flow conditions. Valve defects prevent efficient opening of leaflets resulting in aortic stenosis – causing a high velocity jet of blood flow at the valve orifice – and increased transvalvular pressure gradients (TPG) which is associated with heart attack [4]. Both of these parameters are critical for diagnosis of aortic conditions.

Critical analysis of disturbed flow is essential for safe and effective therapeutics since cells in the cardiovascular system are particularly susceptible to mechano-biological triggers resulting in upregulation or downregulation of gene expression and changes in various biological mechanisms leading to further complications [5]. Currently, diagnosis of aortic defects depends heavily on doppler echocardiography, which has been associated with significant errors in calculation of disease parameters such as TPG or cross sectional area of jet flow due to simplifying assumptions and inaccuracy of measurement [6]. Thus, computational fluid dynamics has emerged as an alternative approach for elucidating complex hemodynamical flows where clinical measurement schemes are limited. In particular, fluid structure interaction (FSI) approaches can be used to more reliably model the dynamicity of leaflets and blood flow throughout the cardiac cycle.

When aortic valve leaflets are damaged beyond repair, surgeons and patients are often left with two choices for replacement of the valve. One option is to replace the damaged valve with an artificial mechanical valve. The benefits of a mechanical valve include long term durability due to the strength of the material, but they are known to provide surfaces where blood can clot more easily. As a result patients with mechanical valves must be kept on life long blood thinners in order to avoid blood clots [7]. The other option is to replace the aortic valve with the pulmonary valve in a procedure known as the Ross procedure, the impetus being that the pulmonary valve undergoes less stress on a daily basis and thus could better handle a graft replacement[1]. The Ross procedure has shown long-term clinical success but involves a more complicated surgical procedure which few surgeons are familiar with and which may potentially create a two valve disease out of a one valve disease [8]. Literature provides inconclusive results about the long-term success of these treatment options with certain studies showing the Ross procedure associated with lower all-cause mortality compared with mechanical aortic valve replacement while other studies suggest that there is no significant difference between the two or perhaps slightly better outcomes with the mechanical valve when optimal anticoagulation therapy is also applied [8-10]. Thus there is a need for further investigation as to the efficacy of each treatment option. In this project, we seek to study the hemodynamical differences between the pulmonary valve and the mechanical aortic valve geometries under the normal physiological stresses of the aortic valve. Using computational modeling for each of these treatment options, a method which has largely been ignored to this point, we hope to gain insight as to the long term replacement success of both mechanical and pulmonary valves under aortic conditions (pressure and flow velocity). We focus on adult implants due to the complexity of pediatric aortic valve replacement and changing aortic geometries with growth of pediatric patients. We hypothesized

[1] This information was obtained in conversation with cardiothoracic surgeons at the Aswan Heart Center in Aswan, Egypt

that due to the pulmonary valve's semilunar geometry and elastic biomaterial, the Ross-procedure is the preferable option for valve replacement as measured by hemodynamic indicators such as maximum jet velocity, maximum transvalvular pressure gradient (TPG), as well as structural indicators such as wall shear stress (WSS), and von Mises stress on the leaflets.

II. Methods

In this study, we simulated aortic valve hemodynamics using COMSOL Multiphysics in combination with aortic anatomy derived from patient specific echocardiography found in literature and boundary conditions both taken from literature and measured from patient specific data with permission from the Magdi Yacoub Foundation and the Aswan Heart Center in Aswan, Egypt. Fluid-Structure Interaction with laminar flow and solid mechanics was used for the simulation of both the pulmonary valve simulation and the mechanical valve.

2.1 Geometries

In order to simulate the blood flow through the two valves, a 2D model geometry was generated based on valve dimensions found in the literature. For the pulmonary valve we derived valve dimensions from echocardiography imaging of a healthy individual [11]. Emulating this geometry, we first created a rectangular domain to emulate the channels upstream (on the left ventricular side) and downstream (aortic side) of the valve and expanded the outlet slightly to emulate aortic expansion during systole. In constructing the aortic root, we added leaflets using the Quadratic Bezier tool. Downstream of the leaflets, two additional cavities were constructed in order to replicate the pulmonary valve's sinuses of valsalva using the parametric curve $\frac{1}{3} R \sin(\pi/2 * R * s)$. The aortic root and leaflets are symmetric with an arterial diameter of 2.4 cm and a total computation domain of 6 cm in length. This structure field consists of rigid walls, including the aortic root, with the no-slip boundary condition applied. The leaflets, however, are flexible with fixed points at the joints between the leaflets and the aortic wall in order to model the opening of the valve as the flow progresses.

The mechanical valve geometry was modeled after the commercially available SJM Regent™ Mechanical Heart Valve, a bileaflet aortic valve replacement device that has emerged as one of the most commonly implanted replacements of heart valves [14]. To simulate the replacement of valves into the same aorta, the aortic wall that was constructed for the previous geometry was used for this model as well, but with the mechanical leaflets instead of the pulmonary leaflets. To model the two mechanical leaflets, two rectangles with side lengths 1.2 cm and thickness 0.1 cm were created. These rectangles were then rotated 25º and -25º respectively to create a v-shaped structure pointing toward the aortic inlet [13]. Two circles of radius 0.03 cm were then constructed and placed inside the rectangles with a total distance of 3mm between each to mimic the hinge joint for each of the two leaflets. These circles were defined as Rigid Connectors to create an axis about which the rectangular leaflets will rotate.

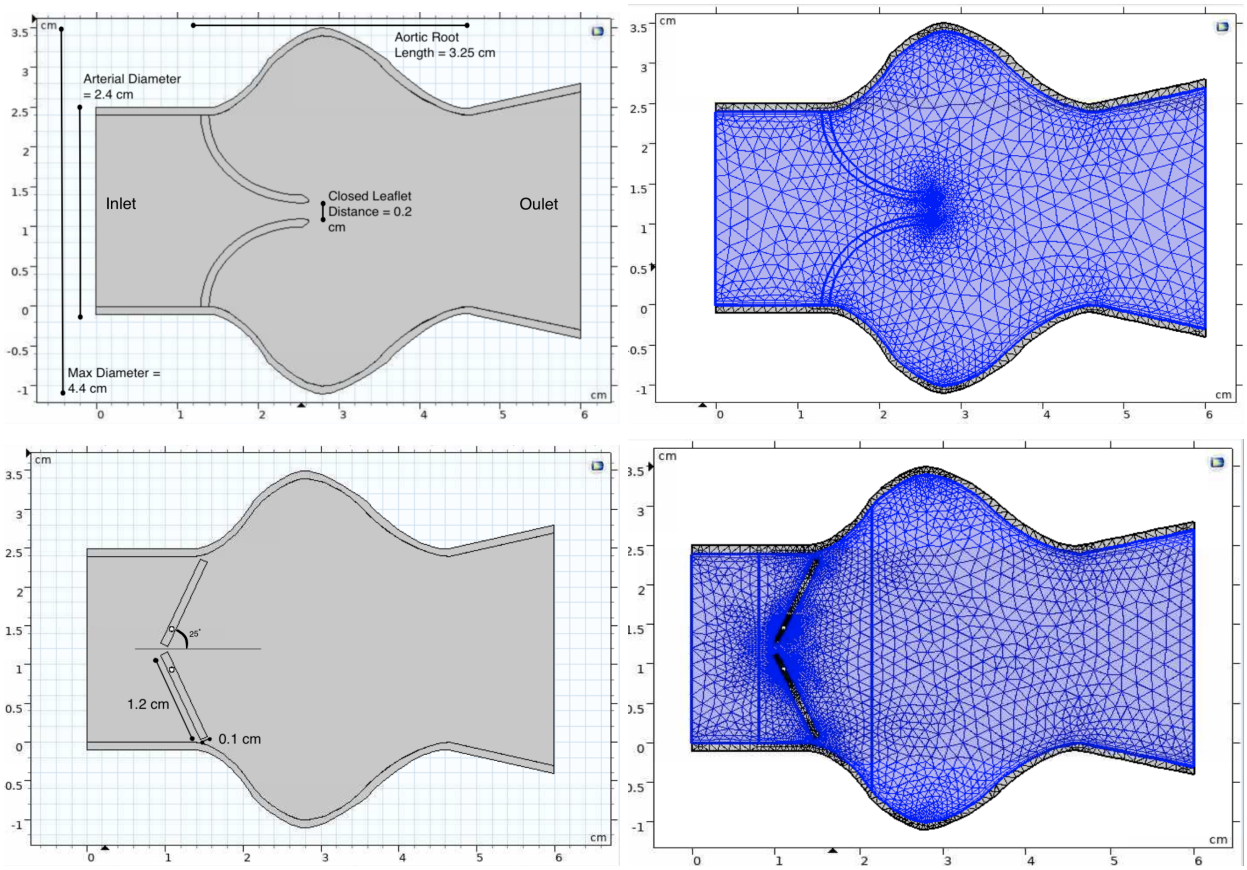

Figure 1. Valve geometries for both pulmonary and mechanical leaflets. (a) shows geometry and dimensions for the pulmonary valve. (b) shows meshing for pulmonary valve with fine mesh near leaflets and walls. (c) shows geometry of mechanical valve. (d) shows meshing for mechanical valve with fine mesh near leaflets and walls and corner refinement on leaflets.

2.2 Materials and Boundary Conditions

The pulmonary valve leaflets and the aortic wall were modeled using a nearly incompressible linearly elastic material with a Young's modulus of 0.37 and a Poisson ratio of 0.49 as described for a healthy tricuspid valve in the literature [11]. Conversely, for the mechanical valve model, the aortic root and wall was still constructed with the same linear elastic material, but the valve leaflets were modeled with a Young's modulus of 30.5×10^9 N/m^2, a Poisson ratio of 0.3, and a density of 2116 kg/m^3 which we found in the literature specifications for the St. Jude Medical bileaflet mechanical heart valve [13]. For modeling of the fluid we created a blood material which we assumed to be incompressible, homogenous, and Newtonian with a constant density of 1060 kg/m^3 and a dynamic viscosity of 0.005 N*s/m^2 throughout the cardiac cycle. Under these conditions, the Navier-stokes and continuity equations govern our fluid flow:

$$\rho\frac{\partial \mathbf{u}}{\partial t}+\rho(\mathbf{u}\cdot\nabla)\mathbf{u}=-\nabla p+\mu\nabla^2\mathbf{u} \qquad (1)$$

$$\nabla\cdot\mathbf{u}=0 \qquad (2)$$

To allow for realistic results, we originally fitted an interpolation function to real-time patient heart pressure data obtained from a healthy patient that we measured at the Aswan Heart Center to use as an inlet boundary condition (Figure 2a). However, the data collected did not work in closing the valve properly due to the thinness and sharpness of its peak. Instead, we turned to an idealized pulsatile velocity waveform published in the literature for the inlet boundary condition of an aortic valve (figure 2b) [12].We recapitulated this profile manually via an interpolation function fitted with a cubic spline curve. The outlet was defined as pressure and set to a gauge pressure of zero. The same inlet profile and outlet setup was used for both pulmonary and mechanical valves.

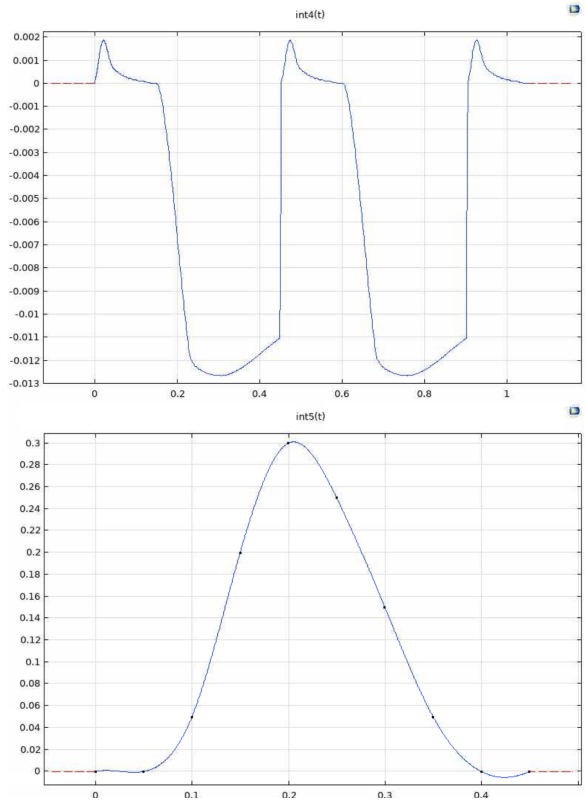

Figure 2. (a) Pressure inlet profile collected from healthy patient heart at Aswan Heart Center. (b) Idealized velocity inlet profile that we ended up using.

2.3 Meshing

We defined the computational domain as a deforming domain with a moving mesh in order to account for the fluid structure interaction. Because leaflet movements are within the flow domain, the flow domain must be re-discretized with each time step to account for moving leaflets. The fluid zone and structure zone were meshed separately. We generated a free triangular mesh (the default in COMSOL). We then applied a fine element with a higher density mesh near the leaflets and walls to capture high velocity gradients. We also implemented corner refinement for enhancing the results at the valve corners and a coarse element for the downstream and upstream fluid to reduce the running time. For the mechanical valve we defined a smaller area around the leaflets, in particular, to reduce the deforming domain and the processing time (see figure 1d). Our approach makes use of the Arbitrary Lagrangian-Eulerian (ALE) formulation, commonly used in bileaflet valve simulations, to ensure higher solution accuracy due to the simultaneous boundary displacement for both the fluid and structure domains.

2.4 FSI Coupling and solver specifications

We used a fully-coupled FSI to model the pulmonary valve. As with most valve FSI simulations we used COMSOL to solve laminar flow of the fluid, in a Single Phase Flow interface, and the solid mechanics of the valve, in a Solid Mechanics interface, separately. We then coupled the two in a Fluid Structure Interaction interface using an ALE method to combine the Eulerian description of fluid flow and the Lagrangian description of the solid. We used a fully coupled specification in our FSI (commonly regarded to have the best accuracy) to compute the leaflet motion based on the solution from the fluid domain with the same timestep. The same specifications were applied to the mechanical valve to simulate its range of motion from 25^{o} to 85^{o} with the top leaflet rotating clockwise and the bottom leaflet rotating counterclockwise.

Finally, for solver specifications, we used a time dependent solver in which the total solution time was 0.4 s to capture complete opening and closure of the valve. The total time was divided into time steps of size 5e-03 s.

2.5 Data Collection

Post-processed results included measurements of jet velocities and TPG in the simulation with the pulmonary valve. The jet velocity for the pulmonary valve was found by creating a 2D cutline along the horizontal centerline of the geometry on which data was extracted and plotted against the length of this cutline for each timestep, and the TPG was found by comparing the gauge pressure on the inlet side to the fixed pressure of 0 Pa at the outlet. The maximum value for all timesteps was documented in Table 1 below. For the mechanical valve, however, two additional orifices had to be considered since blood flows both in between the two mechanical leaflets as well as in between each leaflet and the aortic wall. To account for this, the maximum velocity for each timestep was compared manually across the entire surface and the maximum was documented in Table 1. Sophisticated methods for automation of this process exist but given the number of data points to compare, it was deemed inefficient to construct these complicated methods as it would most likely take longer than comparing the data manually. Vorticity for both simulations was plotted on the 2D surface of the geometry and compared manually as well.

Wall shear stresses which essentially represents the frictional force along a wall were found for the aortic wall as well as the leaflets by using the formula:

$$WSS = \mu \nabla u \qquad (3)$$

where u represents the velocity and μ is the dynamic viscosity [11]. Research showed that this can be implemented in COMSOL by taking the product of the shear rate spf.sr and the dynamic viscosity spf.mu [16]. The maximum values for these were documented in Table 1 and the averages were found by exporting the data for all timesteps and importing it to a python script which performed the necessary arithmetic to find the averages. Internal shear and Von Mises

Stresses for the leaflets were found as well using the built-in expressions solid.mises and solid.stt in COMSOL.

III. Results

The primary results for valve assessment will focus on hemodynamics and shear stress around valve geometries. In particular, velocity distribution and transvalvular pressure gradient are common measures for valve performance, and wall shear stress is a metric for both damage to blood and the epidcardial lining of the aortic wall. Secondary results will look at leaflet dynamics and positions throughout the cardiac cycle and maximum von Mises stress distributed within the valve leaflet. Clinical interpretations will be discussed in the discussion section.

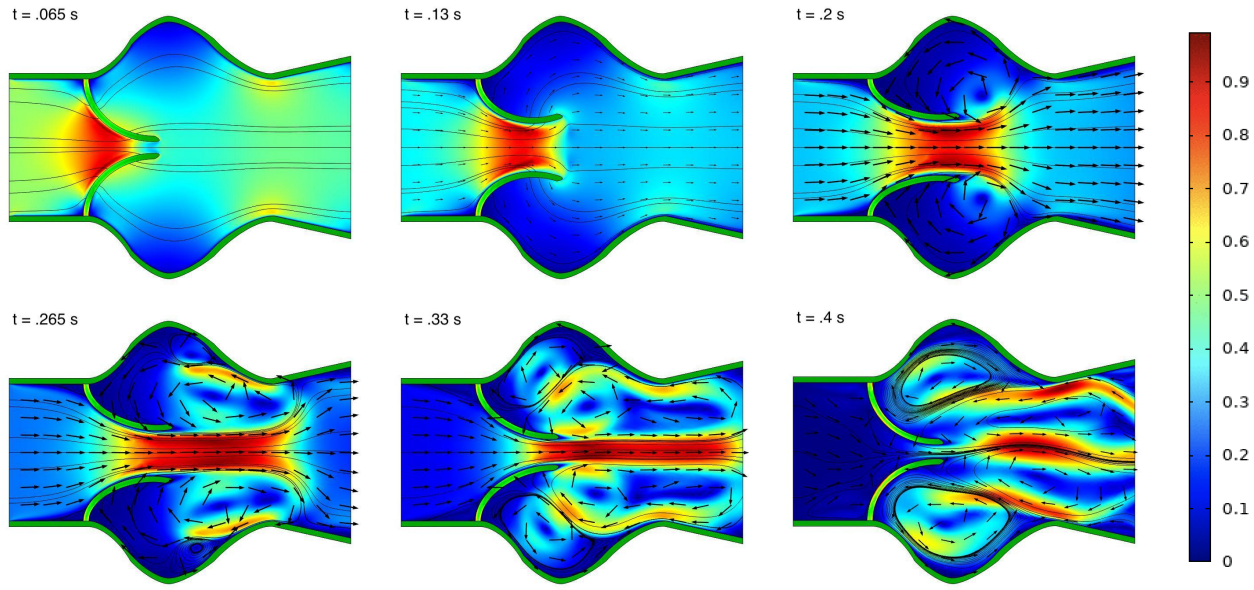

Figure 3. Velocity streamlines and contours for the pulmonary valve implant at various time points throughout the cardiac cycle. We can clearly see high velocity jet flow at systole and circulatory flow in the sinuses during late cycle. This mimics the flow patterns of the aortic valve.

Figure 3 shows snapshots of the velocity contours and streamlines for the pulmonary valve implant. The cardiac cycle begins with a buildup in pressure from 0.05 - 0.1s representing filling of the left ventricle. Ventricular contraction then occurs causing larger jumps in pressure and opening of the valve leaflets. Peak systole occurs between 0.185 - 0.2s characterized by the maximum transvalvular pressure of 302 Pa, maximum jet velocity of 0.93 m/s, and maximum orifice diameter of 12 mm which is similar to that of a healthy aortic valve [15]. During this time, the blood flow follows a plug flow profile with maximum velocity localized at the center of the jet. Valve leaflet deformation also occurs between 0.15 - 0.20s as would be seen in a real aortic valve [15]. Streamline patterns also reveal circulatory flow in valve sinuses. For $t > 0.2s$, as the valve begins to close, unidirectional vorticity is evident indicating unidirectional (not

oscillatory) wall shear stress on the back fibrosa side of the leaflets as has been confirmed by previous studies for ordinary aortic valve leaflets [3]. The shear stresses found for this valve were lower than expected for both the wall shear stress at the valves and along the aortic wall throughout the aortic root (see Table 1). Von Mises stress increased with flow velocity reaching a maximum $7.2x10^4$ Pa on the front ventricularis side of the leaflets and a maximum of $4.9x10^4$ Pa on the back fibrosa side. The maximum magnitude of the vorticity reached 4861 rotations per second and large symmetric vortical rings were clearly visible. In comparison to literature, the pulmonary valve implant appeared to be behaving in a similar manner to a mildly calcified aortic valve with less TPG and WSS although these depend, in part, on the particular inlet velocity profile used for the model [15].

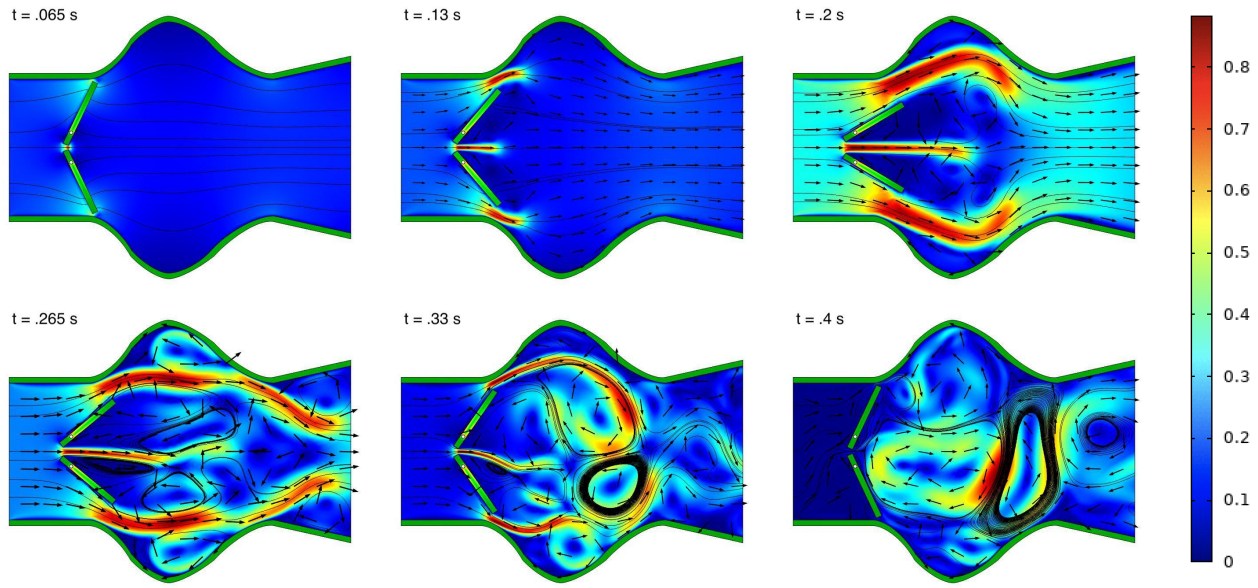

Figure 4. Velocity streamlines and contours for the mechanical valve implant at various time points throughout the cardiac cycle. We can clearly see high velocity jet flow at systole at the three orifices with transient and disorganized circulatory flow.

Blood flow through the mechanical valve followed a more complex and unrecognizable pattern. For the mechanical valve there are three orifices of smaller diameter through which blood flows throughout the cardiac cycle. The valve begins to open at 0.07s as pressure continuously rises on the ventricular side until 0.13s at which point the valve leaflets open more rapidly. Three jets of blood flow are evident and the cardiac cycle approaches peak systole. The valve remains fully opened with a maximum transvalvular pressure and velocity from 0.2s to 0.23s after which it begins to close again. Circular flow is evident throughout the aortic root in a disorganized fashion.

The maximum jet velocity found in the central orifice is 0.881 m/s which matches the experimental data collected by the ViVitro Lab at the University of Victoria (max velocity of 0.8 m/s for mechanical valve) which we used as a reference when constructing our model [13]. The mechanical model experiences less WSS and Von Mises stress on the leaflets suggesting longer leaflet durability which is also expected (Table 1). WSS on the aortic wall was slightly higher,

however. The maximum TPG was higher for the mechanical valve at 371 Pa and large pressure spikes were visible at the orifices. Maximum vorticity magnitude was also larger at 5743 rotations/s but vortices appeared transiently and were less organized.

Table 1

Extracted results for valve hemodynamics and shear stresses

	Pulmonary Valve	**Mechanical Valve**
Maximum jet velocity	.93 [m/s]	.881 [m/s]
TPG	302 [Pa]	389 [Pa]
Vorticity Magnitude	4861 [rad/ s]	5700 [rad/s]
Max WSS on Aortic Wall	24.3 [Pa]	29.63 [Pa]
AVG WSS on Aortic Wall	3.18 [Pa]	2.85 [Pa]
Max WSS on Leaflet	9.11 [Pa]	7.37 [Pa]
AVG WSS on Leaflet	3.44 [Pa]	2.46 [Pa]
Shear Stress front	38885 [Pa]	13849 [Pa]
Shear Stress back	22037 [Pa]	12562 [Pa]
Von Mises Stress front	71506 [Pa]	24103 [Pa]
Von mises back	49409 [Pa]	21889 [Pa]

IV. Discussion

4.1 Jet Velocity and TPG - similarity to AS LSHG patients

As seen in Table 1, the maximum jet velocity measured in the simulation with the pulmonary valve reached approximately .93 m/s while the highest measured velocity for the mechanical valve only reached approximately .88 m/s in a smaller orifice diameter. For validation purposes, this data was compared to clinical reference points which showed that the maximum jet velocity for a healthy individual should reach approximately 1 m/s, and the results were thus concluded to be sufficiently accurate for further analysis [17]. Furthermore, the TPG in the simulation for the mechanical valve was 389 Pa, compared to the TPG with the pulmonary valve which was 302 Pa. Together, these jet velocities and the pressure gradients provide reasons

for considering patients with mechanical valve implants similar to those in a particular group of aortic stenosis patients, namely those with Low Flow, High Gradient (LSHG) characteristics. This group has been shown to experience an imapired cardiac output as well as a partially decreased longitudinal function of the left ventricle [17]. Previous literature also emphasizes the relationship between increased TPG and heart attacks which means that the TPGs measured in this study suggests that recipients of mechanical heart valves may suffer greater risks of experiencing an infarction [15]. This conclusion is in agreement with previously mentioned studies.

4.2 Wall Shear Stress and Von Mises Stress

Concerns with the pulmonary valve include accelerated calcification of the leaflets over time due to the higher Von Miss and Wall Shear stresses on the leaflets particularly at the base and at the center of the front ventricularis side of the leaflet respectively. Calcification is known to cause aortic stenosis characterized by increased TPG and decreased orifice diameter [15]. The mechanical valve does not face the same concern due to its high young's modulus and yield stress which is resistant to degradation. The mechanical valve also experiences less wall shear stress and Von Mises stress on its leaflets due to its geometry and freer rotation. This suggests longer durability for the mechanical valve, which was expected.

In addition to stress on the leaflets, however, high wall shear stresses have long been known to cause endothelial dysfunction by damaging the inner layer of the aortic wall. In this study, we found that wall shear stress on the aortic wall was actually slightly higher for the mechanical valve than the pulmonary valve, likely due to the proximity of the top and bottom orifices and jets to these walls. The magnitude of this increase is not large enough to disrupt the flow or cause immediate damage to the aorta, but may cause future complications related to endothelial dysfunction over time, especially since mechanical valves typically are chosen for their durability when operating in young patients.

4.3 Vorticity

The extent and strength of vortical motion surrounding the mainstream is an important consideration. Reduced strength of vortices may have notable clinical implications. Rotation in the bloodstream may naturally cause gentle scouring of the endocardial and endothelial lining of the aortic wall and reasonable amounts are necessary. Reasonable amounts of this can keep blood elements suspended (stirring of blood components). Its weakening may therefore contribute to thrombus formation (blood clotting phenomena). Not only might vortical flow have bearing on the avoidance of thrombosis, but also, by being responsible for swirling flow it contributes to avoidance of atherogenicity (formation of abnormal fatty or lipid masses in arterial walls). When too strong, however, vorticity can damage the endocardial and endothelial cells causing cellular dysfunction. The pulmonary valve model displays adequate vorticity strength (max of

4861 rad/s) in an organized and controlled fashion without exerting too much force on the aortic walls. Its vortical patterns mimic closely that of the aortic valve and it relies on vorticity for closing. The mechanical valve, however, has a higher maximum vorticity magnitude and its vortical pattern is more transient and disorganized which may actually damage blood elements and the aortic root. Thus, we believe that the pulmonary valve vorticity exhibits healthier valve behavior under aortic conditions.

4.4 Conclusion

Due to hemodynamic characteristics more closely mimicking a healthy aortic valve, and due to the need for lifelong anticoagulation medication when treated with a mechanical valve, we recommend the Ross procedure as the ideal aortic valve replacement option for patients suffering from aortic valve defects. Of course, clinical decisions vary and depend heavily on the individual patient and their respective circumstances. In the case of a young-adult patient, for example, where durability is more of an important factor for long term success, the mechanical valve might be more advantageous such that the young patient does not need further corrective surgery and can avoid future surgical complications. Likewise, if the patient has a weak pulmonary valve then the mechanical valve must be used. However, our work serves as an idealized model to demonstrate the proof of concept of using CFD and FSI to make clinical decisions based on patient derived data. We hope to provide an impetus for use of CFD in surgical decision making which is still largely ignored to this point.

4.5 Limitations

There are several limitations to our methodology that curb the clinical applicability of our models. On the one hand our simulation is in 2D which misses out on the precise tricuspid geometry of the pulmonary valve. We chose to do a 2D model due to the limitations of COMSOL, the immense computing power required for 3D FSI, and the limitations of our own experience. Nonetheless, 2D models have been shown to be useful for clinical examination of aortic valve defects. We have also kept the aortic root stationary, applying FSI computations to the leaflets only. In reality, the aortic root has been shown to change by as much as 10% in diameter during systole to assist in the ejection of blood [18]. This, of course, limits the accuracy of our simulation. With regards to geometry, the geometry we created for the mechanical valve was simplified for purposes of achieving a functional FSI simulation. For example, we used a pin hinge instead of the actual butterfly hinge found in an actual mechanical valve. Furthermore the rotation about this pin hinge partially depends on the inlet velocity profile which likely affects the actual flow behavior and stresses that would appear in a mechanical valve. For the pulmonary valve model, valve leaflets in an actual biological valve (and in more accurate FSI models) have been shown to deform more than we have shown upon opening which we have not recapitulated here due to the difficulty of this FSI calculation. In addition, we have applied a uniform linear

elastic material to our valve leaflets which is unrealistic given the non-homogenous calcification of valve leaflets in the human body. Likewise, the dynamicity of leaflet calcification over time due to shear stress response would be difficult to model. Finally we had no means of validating our model against consistent patient data as would be ideal in a clinical setting where leaflet deformation would be compared to actual echocardiography imaging for patient-specific modeling and analysis of leaflet orientation during ventricular systole and diastole. Ideally, we would also have the proper inlet pressure profile data for the patient whose valve we were modeling. In this study, however, an idealized velocity profile was obtained from relevant literature and used. Thus, we cannot be sure as to the precise accuracy of our model for the given dimensions. We see this in the fact that some of our results are not in line with expected aortic valve values such as our vorticity measurements which were much higher than published aortic valve values for both implant options.

4.6 Future Directions

With this basic 2D model, many more valve characteristics can be tested for their effects on blood flow (this is the beauty of computational modeling)! We could test several other leaflet geometries varying the extent of curvature to assess optimal geometry for blood flow. We could also test for asymmetries in the leaflets to see how this might affect blood flow which would be an effective mode of disease modeling. For patients with bicuspid aortic valves, asymmetric leaflets are a common defect. Finally, we could also test the effects of calcification on the leaflets by adjusting the young's modulus of the material used to create the aortic valve. Studies have shown that increased calcification causes higher velocity of flow and higher pressure gradients resulting in more strain on the heart [15].

Ultimately, we have seen how computational fluid dynamics and modeling have emerged as powerful tools for planning clinical interventions and improving outcomes. Although here we chose a generalized approach, the power of CFD can be fully realized in patient-specific modeling for achieving truly personalized medicine. This study serves largely as a proof of concept, and decisions for optimal treatment options must be patient specific.

V. References

[1] Virani SS, Alonso A, Benjamin EJ, Bittencourt MS, Callaway CW, Carson AP, Chamberlain AM, Chang AR, Cheng S, Delling FN, Djousse L, Elkind MSV, Ferguson JF, Fornage M, Khan SS, Kissela BM, Knutson KL, Kwan TW, Lackland DT, Lewis TT, Lichtman JH, Longenecker CT, Loop MS, Lutsey PL, Martin SS, Matsushita K, Moran AE, Mussolino ME, Perak AM, Rosamond WD, Roth GA, Sampson UKA, Satou GM, Schroeder EB, Shah SH, Shay CM, Spartano NL, Stokes A, Tirschwell DL, VanWagner LB, Tsao CW; American Heart Association Council on Epidemiology and Prevention Statistics Committee and Stroke Statistics Subcommittee. Heart Disease and Stroke Statistics-2020 Update: A Report From the American Heart Association. Circulation. 2020 Mar 3;141(9):e139-e596. doi: 10.1161/CIR.0000000000000757. Epub 2020 Jan 29. PMID: 31992061.

[2] Maleki H. Structural and fluid-structure interaction analysis of stenotic aortic valves: application to percutaneous aortic valve replacement. Concordia University; 2010.

[3] Yap CH, Saikrishnan N, Tamilselvan G, Yoganathan AP. Experimental measurement of dynamic fluid shear stress on the aortic surface of the aortic valve leaflet. Biomech. Model Mechanobiol 2012;11(1–2):171–82.

[4] Otto CM, Prendergast B. Aortic-valve stenosis — from patients at risk to severe valve obstruction. N Engl J Med 2014;371(8):744–56.

[5] Winslow RL, Trayanova N, Geman D, Miller MI. Computational medicine: translating models to clinical care. Sci Transl Med 2012;4(158):158rv11. 158rv11.

[6]Shadden SC, Astorino M, Gerbeau JF. Computational analysis of an aortic valve jet with Lagrangian coherent structures. Chaos 2010;20(1), 017512.

[7] Zakaria, M. S., Ismail, F., Tamagawa, M., Aziz, A. F. A., Wiriadidjaja, S., Basri, A. A., & Ahmad, K. A. (2017). Review of numerical methods for simulation of mechanical heart valves and the potential for blood clotting. *Medical & biological engineering & computing*, *55*(9), 1519-1548.

[8] Mokhles, M. M., Körtke, H., Stierle, U., Wagner, O., Charitos, E. I., Bogers, A. J., ... & Takkenberg, J. J. (2011). Survival comparison of the Ross procedure and mechanical valve replacement with optimal self-management anticoagulation therapy: propensity-matched cohort study. *Circulation*, *123*(1), 31-38.

[9] Mazine, A., Rocha, R. V., El-Hamamsy, I., Ouzounian, M., Yanagawa, B., Bhatt, D. L., Verma, S., & Friedrich, J. O. (2018). Ross Procedure vs Mechanical Aortic Valve Replacement in Adults: A Systematic Review and Meta-analysis. *JAMA cardiology*, *3*(10), 978–987. https://doi.org/10.1001/jamacardio.2018.2946

[10]Mazine, A., David, T. E., Rao, V., Hickey, E. J., Christie, S., Manlhiot, C., & Ouzounian, M. (2016). Long-term outcomes of the Ross procedure versus mechanical aortic valve replacement: propensity-matched cohort study. *Circulation*, *134*(8), 576-585.

[11] Torrado, A., Sequeira, A., Tiago, J., & Pinto, F. Analysis of hemodynamic indicators in Bicuspid Aortic Valves using a computational mathematical model.

[12] Bloomfield P.. Choice of heart valve prosthesis. *Heart (British Cardiac Society)*, *87*(6), 583–589. https://doi.org/10.1136/heart.87.6.583
[13] Yeh H. Computational analysis of fluid structure interaction in artificial heart valves. *University of British Columbia Theses.* https://open.library.ubc.ca/cIRcle/collections/ubctheses/24/items/1.0074167
[14] Caballero, A. D., & Laín, S. (2015). Numerical simulation of non-Newtonian blood flow dynamics in human thoracic aorta. *Computer methods in biomechanics and biomedical engineering*, *18*(11), 1200-1216.
[15] Amindari, A., Saltik, L., Kirkkopru, K., Yacoub, M., & Yalcin, H. C. (2017). Assessment of calcified aortic valve leaflet deformations and blood flow dynamics using fluid-structure interaction modeling. *Informatics in Medicine Unlocked*, *9*, 191-199.
[16] Comsol Forum. https://www.comsol.com/forum/thread/83661/wall-shear-stress
[17] Chaothawee, Lertlak. (2012, 12, 12). *Diagnostic approach to assessment of valvular heart disease using magnetic resonance imaging, part II: a practical approach for native and prosthetic heart valve stenosis.* US National Library of Medicine. https://www.ncbi.nlm.nih.gov/pmc/articles/PMC4832612/#:~:text=Forward%20flow%20velocity%20measurement&text=Peak%20velocity%20of%20forward%20flow,m%2Fs%20in%20severe%20stenosis.
[18] RG1 Leyh, Schmidtke C, Sievers HH, Yacoub MH. Opening and closing characteristics of the aortic valve after different types of valve-preserving surgery. Circulation 1999;100(21):2153–60.